A preliminary urban seismic risk model for the City of Rhodes Greece

Karaferi Evdoxia – National Technical University of Athens, Athens, Greece, e-mail: ekaraferi@mail.ntua.gr

Melissianos Vasileios – National Technical University of Athens, Athens, Greece, e-mail: melissia@mail.ntua.gr

Vamvatsikos Dimitrios – National Technical University of Athens, Athens, Greece, e-mail: divamva@mail.ntua.gr

Abstract: A first-order model is developed for the seismic risk assessment of the water supply network and the structural integrity of the buildings of Rhodes under spatially correlated seismic loading. For its implementation, in-house software is coded in the object-oriented programming language Python. The water supply network is modelled via a graph theory approach and the vulnerability of the buildings takes advantage of the 2020 European Seismic Risk Model. An event-based probabilistic seismic hazard approach is employed, generating ground motion fields for 10,000 years with the OpenQuake platform. The intensity measures used are the peak ground velocity (PGV) for the water pipelines and Sa(1s) for the buildings. The close correlation of the two allows the creation of spatially cross-correlated PGV and Sa(1s) values that are otherwise not readily available. Results are obtained, per block, for the percentage of people that have no access to water and for the damage of buildings. This is enough to offer a preliminary determination of the disruption caused by each event in terms of available housing and utilities, in support of socioeconomic impact modeling.

Keywords: Fragility curves, Vulnerability functions, Ground motion fields, Losses, Cost

1. Introduction

Risk assessment is a rapidly evolving field in engineering with more and more attention brought towards it, in an attempt to define and control, as much as possible, the effects of a catastrophic event. Risk assessment models can be applied to a variety of infrastructure and lifeline systems and used for multiple natural hazards, from earthquake to wind or snow. Combining all these data into one risk model can help manage the consequences and facilitate planning proper strategies and measures to effectively prepare, and therefore protect, a city in a time of need. Many studies in the past have dealt with simulating individual parts or utility networks of a city (Winkler et al., 2010; Esposito et al., 2015; Costa et al., 2018). Typically, the difficulty lies in interconnecting said networks (Dueñas-Osorio et al., 2007) and integrating the results from different models onto one full model that correctly aggregates the impact of each system/network on the socioeconomic and business activities of the city.

The EU-funded HYPERION research project (HYPERION, 2019) attempts to create an engine that can assess the risk of all major infrastructure that are important and affect the ability of a city to return to normality after severe natural disasters. In the context of this project, a methodology is being developed that aims in the creation of a realistic all-inclusive urban seismic risk model for the four European cities of Granada (Spain), Venice (Italy), Tønsberg (Norway), and Rhodes (Greece). Herein, a subset of its results is presented for the city of Rhodes, encompassing the buildings and the water supply network. In many ways it is a blueprint of what is being planned as the desired outcome for the project as a total is incorporating all utility networks and the transportation system to be connected to a

socioeconomic model that will eventually allow simulating the functionality of the entire city.

2. Exposure model for the City of Rhodes

For the case study of this preliminary urban model, fundamental infrastructure of the city was studied, herein comprising the water supply network and the building stock. In a touristic city, like Rhodes, the population is multiplied by factors of two or more during the summer months, something that is not taken into consideration; the population considered is only the permanent population of the city.

The water supply system consists of the transmission system and the distribution system. The transmission system brings water from the sources, a dam and a boring site, to the urban distribution network that provides water for the consumers. The topology of the pipelines of the transmission system are known, while for the pipelines of the distribution system it is assumed that they follow the routes of the city streets. The population and building data for the city blocks is taken from the Hellenic Statistical Authority data, ELSTAT (2021) using the latest 2011 Census data. To achieve an efficient risk assessment model, a graph is created for the distribution system with the nodes being the points of water entry (dam, boreholes), the water outlets, and the joints of multiple pipe branches, while the edges represent the pipes.

The census data offers information about the number, the age and the material of the buildings in the city per city block. Due to the complexity of a model that would include all those details, some simplifications were made. To be more specific, the type of buildings that are more probable to appear per block was chosen to represent it and therefore it is assumed that for each block only one building type is taken into consideration. Ultimately, a simplified model is produced where in the old city only masonry structures appear while the rest of the city is represented by reinforced concrete buildings. This assumption leads to more-or-less the same distribution of materials (or building types) over the entire city (Table 2), with a slight heavier concentration of masonry in the cultural heritage downtown than otherwise expected. It is also accepted that each block is represented through its centroid where the total number of the buildings of the block is supposed to be concentrated. The centroid is also the point where each intensity measure is considered to be applied.

Table 1. Percentage of building materials for the city of Rhodes Greece, as provided by ELSTAT and as adopted in the simplified city model

% of material	Actual	Simplified city model
Reinforced Concrete	75.5	82.7
Masonry & Stone	22.9	17.3
Steel	1.1	-
Wood	0.1	-
Other	0.4	-

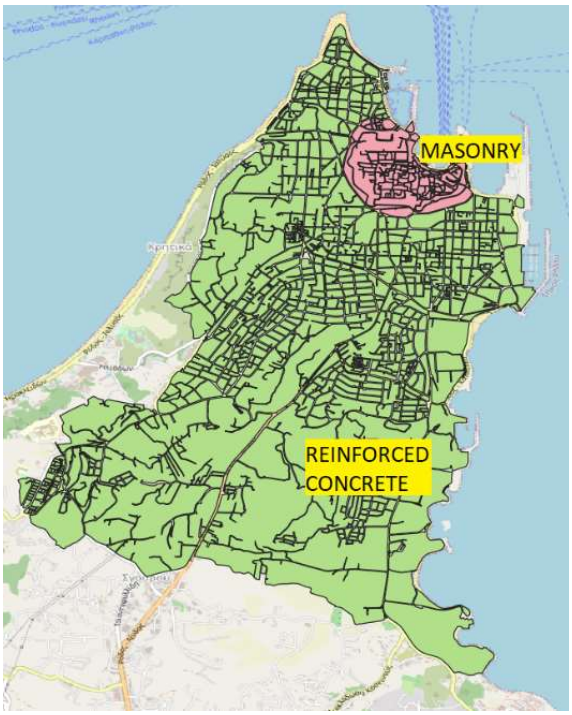

Fig. 1 – Simplified city model and corresponding classification for the buildings of Rhodes

Table 2. Chosen GEM buildings typology specifications chosen

	Typology 1	**Typology 2**
	CR_LFINF-CDM-15_H2	MUR_LWAL-DNO_H2
Material	Reinforced concrete	Unreinforced masonry
Lateral load resisting system	infilled frame	load bearing wall
Code Level	moderate code level	non-ductile
Lateral Force Coefficient	15%	—
Number of stories	2	2

3. Intensity measures

There are multiple intensity measures (IMs) that can be used for urban area studies, such as the peak ground acceleration (PGA), peak ground velocity (PGV) or spectral acceleration (Sa), typically at a period of 0.2s or 1.0s. The type of intensity measure used depends on the type of assets that need to be assessed. For example, one may prefer PGA for lowrise structures and SA(1.0s) for highrise ones, while for the water supply system, PGV is a strong indicator of the possible damages that can occur to the pipelines according to ALA (2001). Generally, the ALA also takes into consideration the permanent ground displacement, but since there are no significant slopes, liquefaction and or important fault displacement for the case study site, this intensity measure is not accounted for.

The problem is that combining different IMs can spell trouble, especially when examining seismic hazard over a whole city instead of a single site. For single sites, classic probabilistic seismic hazard analysis (PSHA) can be employed, its results summarized in familiar hazard curves. For multiple sites over an area, though, the Monte-Carlo-style event-based PSHA is

needed. Essentially, one needs to simulate a stochastic set of potential events over a period of several thousand years, each event matched with a spatially-correlated IM field, e.g. as generated by the OpenQuake engine (GEM, 2021). When multiple IMs are at play, said fields also need to be cross-correlated among the different IMs. At present, spatial correlation functions for PGV are not encoded in OpenQuake, while cross-correlation is not enforced, necessitating a slightly different approach if one wants to tackle both buildings and pipelines.

As a compromise, we chose to use Sa(1s) as our primary IM for two reasons. First, appropriate models for its spatial correlation are available (Jayaram and Baker, 2009). Second, there is a strong correlation of the order of 0.8 between Sa(1s) and PGV (Bradley, 2012). This allows us to essentially copy the correlation structure of Sa(1s) and paste it into the PGV fields. To do so, a single stochastic event catalogue was created, corresponding to a long enough investigation time of 10,000 years. Separate event-based analyses were run for each of the two IMs using an area source model, and employing the same catalogue and mesh. For simplicity, a single ground motion prediction equation by Cauzzi et al. (2014) was employed. For every field, the Sa(1s) values are sorted, e.g. from smallest to largest, as well as the PGV ones. Then, the PGV values are reordered by employing the sorted-to-original mapping of the Sa(1s) vector, so as to correspond to the initial ordering of the latter. In this way, the maximum PGV value appears at the same point where the maximum Sa(1s) value is; similarly, for the second largest and so on and so forth. In Fig. 2 an example of ground motion fields of a single event are presented, portraying the reordering of the PGV values to match the one of the Sa(1s).

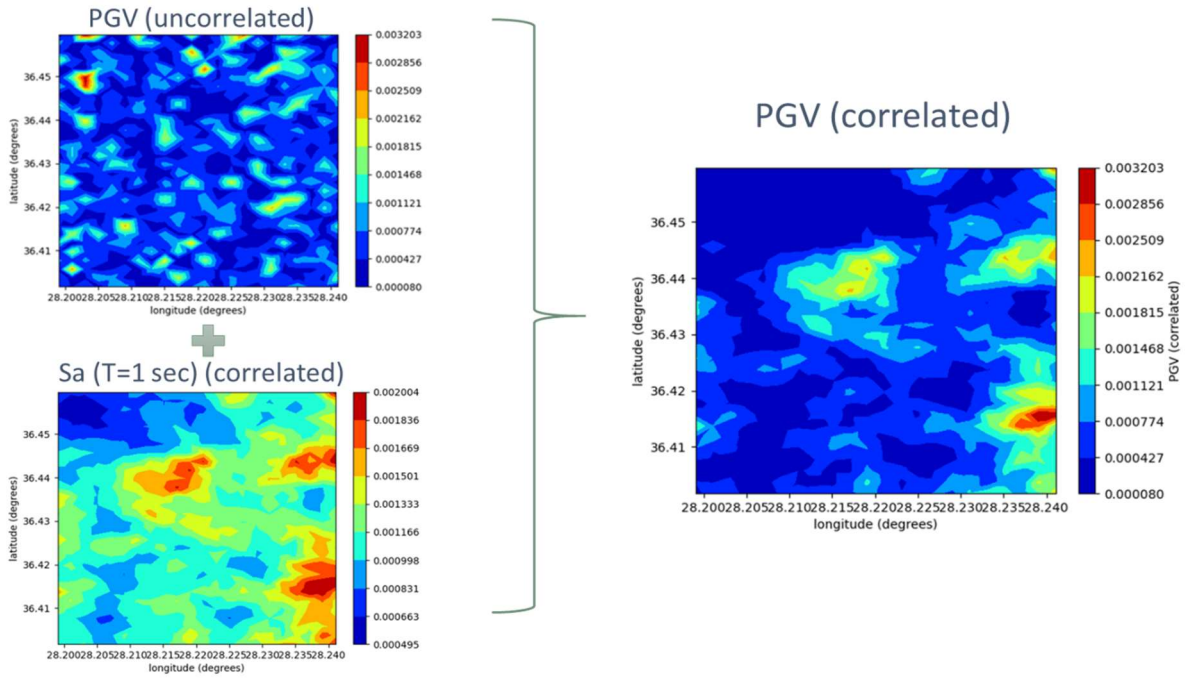

Fig. 2 – Example of the combination of Sa(1s) and PGV fields estimated for a single event to create a PGV ground motion field with spatial correlation

Note that an investigation time of 10,000 years signifies 10,000 different realizations of a single year; therefore a large number of events with negligible impact on the system will appear that will not cause damage to the water pipes. To reduce the computational cost of the analysis, all ground motion fields with a maximum PGV value less than 5 cm/sec are discarded, as they cause no damage. This reduces the events to be considered from about 130,000 to about 2,800 without any loss of accuracy.

4. Fragility/ Vulnerability

4.1. Fragility/ Vulnerability of the water supply network

The methodology used for the seismic assessment of the water distribution (pipe) network is based on the American Lifelines Alliance (ALA, 2001) guidelines. The pipe vulnerability function is given by:

$$RR = K_1 \cdot 0.01425 \cdot PGV \text{ per 100 m of pipe length} \quad (1)$$

where K_1 is based on the pipe material, joint type, diameter, and the soil type. The probability of failure (P_f) for an individual pipeline and a given value of PGV is calculated as:

$$P_f = 1 - e^{-RR \cdot L} \quad (2)$$

where L is the length of the pipe. According to HAZUS-MH (FEMA, 2003), as well as ALA, not all of the failures are breakages; per HAZUS-MH, 20% of such failures are breakages and 80% are leakages. Only breakages require immediate repair, as they stop a pipe from providing at least some water to the residents of the city.

There are two approaches to integrating the damage of individual pipes and assessing their impact at the network level. The first involves solving the system of head-driven differential equations of flow (Cavalieri, 2020; Tomar et al, 2020); this is a computationally expensive but highly accurate approach. The second option focuses on the connectivity of end-users to the water sources via a graph-theory approach (Gibbons, 1985; Fragiadakis et al., 2013); this is considerably more frugal and it is our choice. To create and study the resulting graph model, the python package NetworkX (Hagberg et al., 2008) was used. The overall network system reliability is assessed via the statistics of the considered scenarios, forming in effect a large-scale Monte Carlo simulation.

4.2. Fragility of the buildings

As far as the building stock of the city is concerned, it is important to be able to estimate the losses as well as the risk to completely access the impact of the seismic event (e.g., Kohrangi et al., 2021, Silva et al., 2015). The fragility curves for the buildings are taken from ESRM20 (Crowley et al., 2021). In Table 3 the parameters of the fragility curves are presented, together with the relevant typology of the buildings based on the GEM building taxonomy. To assess damages at each city block and per each event, we use the Sa(1s) value of the field point that is closest to the block centroid. Four limit-states (LSs) are employed to define five damage states and the probability of being in each one.

Knowing the number of buildings in each block as well as the probability of the block to be in each damage state, the number of buildings per block that belong to each damage state can be calculated by multiplying the probability with the total number of buildings in the block.

Table 3. Parameters for the fragility curves from ESRM20 for Sa(1s)

Typology	Median_DS1	Median_DS2	Median_DS3	Median_DS4	Beta
CR_LFINF-CDM-15_H2	0.180	0.259	0.344	0.424	0.531
MUR_LWAL-DNO_H2	0.052	0.166	0.286	0.402	0.869

5. Results

The overall impact to the city can be defined by assessing the percentage of the population that will have to abandon their house due to damage or potentially due to having no access to water. The latter is estimated as the percentage of individual pipes surrounding the block in question that cannot supply water. The developed methodology also allows the allocation of the buildings per damage state for the whole city. Fig. 3 presents three indicative scenario events: (i) An M7.1 event at a distance of 35km, (ii) An M7.9 event at 74km, (iii) a "design level" event that produces the 10% in 50yrs value of Sa(1s) at the center of the city. Results are illustrated in Fig. 4 to 6 in terms of (a) the percentage of population that has access to water per block, (b) the percentage of buildings that are in the DS4 and therefore are completely damaged per block. Clearly, the first two events, which are the strongest in the stochastic catalogue, represent rare extremes, and they end up severely damaging the city. The third is a more reasonable scenario (see the relevant PGA map in Fig. 3b), where moderate building damage is exacerbated by the lack of water supply.

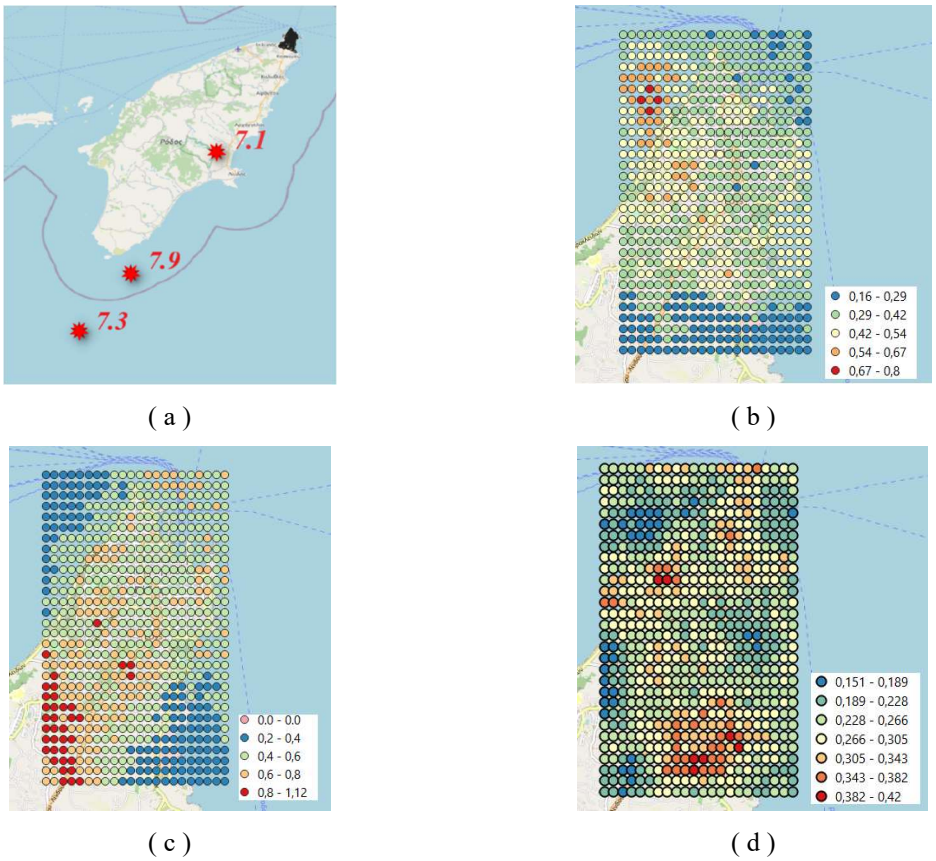

(a) (b)

(c) (d)

Fig. 3 – (a) Map displaying the epicentre of the seismic events presented below with their magnitude. The city itself is shown darkened at the northern tip of the island. (b) M7.9 event at 74km (c) M7.1 event at a distance of 35km (d) M7.3 "design level" event that produces the 10% in 50yrs (d)

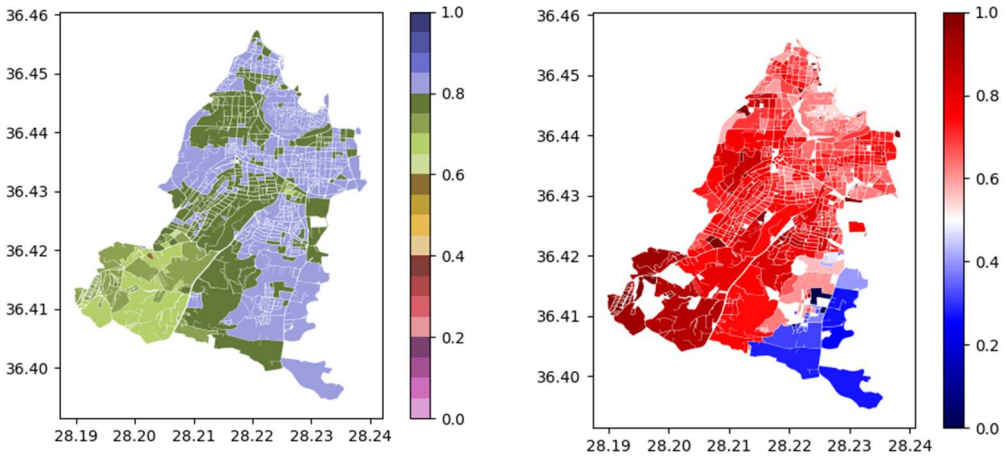

(a) (b)

Fig. 4 – Percentage (a) of access to water and (b) of buildings that collapse per block (M7.1)

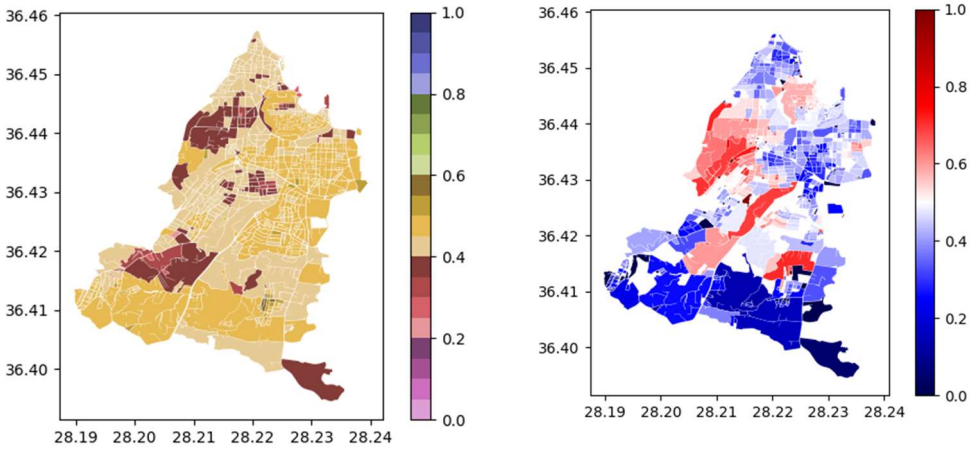

(a) (b)

Fig. 5 – Percentage (a) of access to water and (b) of buildings that collapse per block (M7.9)

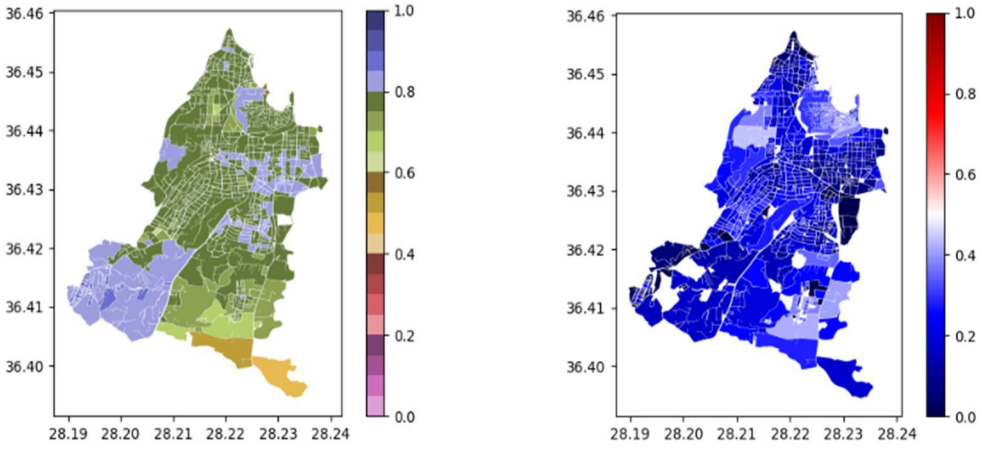

(a) (b)

Fig. 6 – (a) Percentage of access to water, (b) Percentage of buildings that collapse per block (M7.3)

For the chosen typologies of buildings, the losses are calculated from their vulnerability functions and are presented in terms of mean annual frequencies. The vulnerability functions used refer to:

- Total replacement cost vulnerability functions

$$Mean\ loss\ ratio = \frac{cost\ of\ repair}{cost\ of\ replacement} \tag{3}$$

- Occupants vulnerability functions

$$Mean\ fatality\ ratio = \frac{number\ of\ fatalities}{number\ of\ occupants} \tag{4}$$

The mean annual frequency for the loss of life curve is multiplied by the number of occupants to present the number of fatalities (Fig. 7a). The mean annual frequency for the monetary loss represents the amount of an 'average' building that would need to be completely replaced after the event. The number does not actually indicate how many buildings will collapse, but rather what will be the aggregated monetary loss divided by the average replacement cost (Fig. 7b). Finally, Table 4 shows in more detail the statistics of losses from the design level event. Note, that there are fewer masonry buildings that need replacement simply because there are fewer of them overall, as is shown in Table 1. Percentage-wise, masonry buildings remain more vulnerable than reinforced-concrete ones.

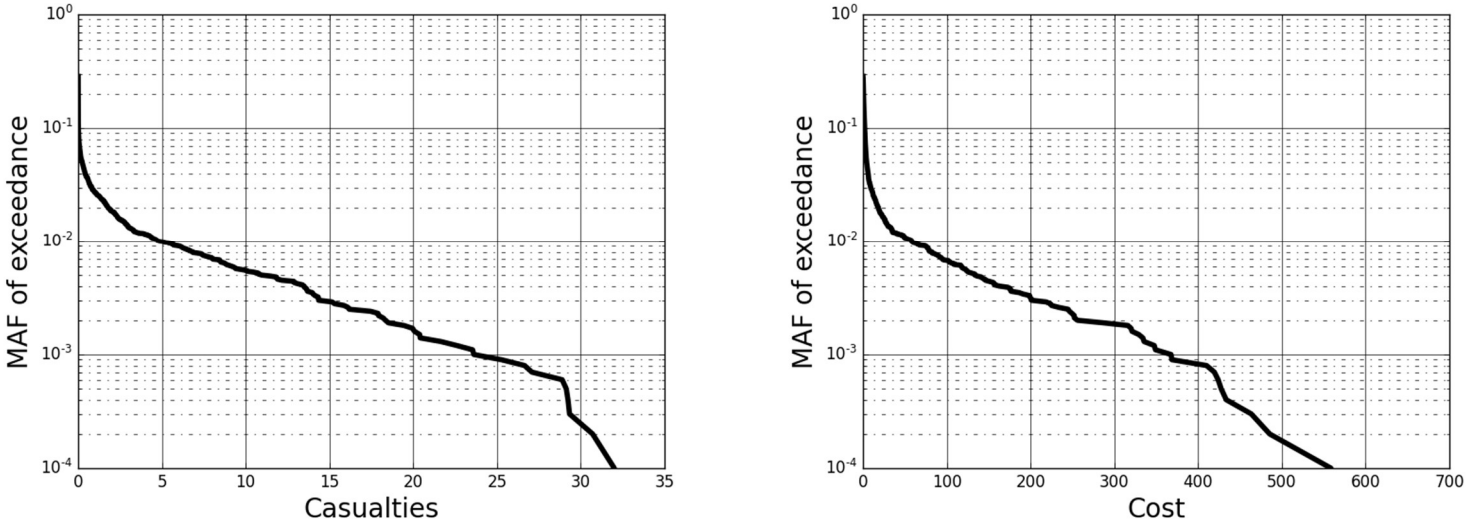

Fig. 7 – (a) Mean annual frequency of exceedance for loss of life, (b) Mean annual frequency of exceedance for the replacement cost

Table 4. Average annual losses and losses from design earthquake, differentiating pipes, masonry (MUR) and reinforced concrete (RC) buildings

			Average Annual Loss	Design Earthquake	
Buildings		Loss of life	0.19	18	
	Replacement cost	Both	2.7	245	2.2%
		RC	1.72	194	2.1%
		MUR	0.98	51	2.6%
Water Network	Percentage of damaged length	Leakages	0.7%	5.8%	
		Breaks	0.2%	1.5%	
	Percentage of failed pipes	Leakages	0.4%	3.6%	
		Breaks	3.2%	0.9%	
	Percentage w/o water		3.2%	6.4%	

6. Conclusions

The methodology developed is an efficient way to assess the risk for a water supply network and the buildings of the given city that accounts for both the topology of the system as well as the spatially correlated seismic intensities. The ALA guidelines are efficiently combined with graph theory and Monte Carlo simulation to provide results for the expected failures that will affect the water supply and the ESRM20 provides the damages inflicted to the buildings and the losses that occurred. The adopted method can take advantage of publicly available data to provide fast computations that combine two major infrastructure types of the city. It gives information about the extent of the failures for the entire system as well as localized information per city block that could be translated into useful results for the number of people that will be affected by a catastrophic seismic event in terms of both housing and accessibility in water. The correlation between the results shows that the most dangerous results for the water system might not be the worst possible for the buildings but the likelihood of simultaneous severe damages in buildings and lack of water is high especially in certain vulnerable parts of the urban grid.

Acknowledgements

Financial support has been provided by the European Framework Programme for Research and Innovation (Horizon 2020) under the “HYPERION” project with Grant Agreement number 821054. Special thanks are also extended to the municipality of Rhodes, the Hellenic Statistical Authority, and the Municipal Water Supply Company of the Municipality of Rhodes (DEYAR) for supplying the data required to build the water supply network model.

References

- ALA (2001). American Lifelines Alliance: Seismic fragility formulations for water systems—guideline and appendices. American Lifelines Alliance, Washington DC, USA. https://www.americanlifelinesalliance.com/Products_new3.htm#WaterSystems
- Bradley, B. (2012). Empirical Correlations between Peak Ground Velocity and Spectrum-Based Intensity Measures. Earthquake Spectra, 28(1), 17-35. https://doi.org/10.1193/1.3675582
- Cauzzi, C., Faccioli, E., Vanini, M., Bianchini, A. (2015). Updated predictive equations for broadband (0.0 - 10.0 s) horizontal response spectra and peak ground motions, based on a global dataset of digital acceleration records. Bulletin of Earthquake Engineering, 13, 1587–1612. https://doi.org/10.1007/s10518-014-9685-y
- Cavalieri, F. (2020). Seismic risk assessment of natural gas networks with steady-state flow computation. International Journal of Critical Infrastructure Protection, 28, 100339, https://doi.org/10.1016/j.ijcip.2020.100339.

- Costa, C., Silva, V., & Bazzurro, P. (2018). Assessing the impact of earthquake scenarios in transportation networks: the Portuguese mining factory case study. Bulletin of earthquake engineering, 16(3), 1137-1163.
- Crowley, H., Dabbeek, J., Despotaki, V., Rodrigues, D., Martins, L., Silva, V., Romão, X., Pereira, N., Weatherill, G., Danciu, L. (2021). European Seismic Risk Model (ESRM20). EFEHR Technical Report 002 V1.0.0, https://doi.org/10.7414/EUC-EFEHR-TR002-ESRM20
- Dueñas-Osorio, L., Craig, J. I., & Goodno, B. J. (2007). Seismic response of critical interdependent networks. Earthquake engineering & structural dynamics, 36(2), 285-306
- ELSTAT (2021). Digital Cartographical Data (DCD). URL: https://www.statistics.gr/digital-cartographical-data [accessed 10/Dec/2021]
- Esposito, S., Iervolino, I., d'Onofrio, A., Santo, A., Cavalieri, F., & Franchin, P. (2015). Simulation-based seismic risk assessment of gas distribution networks. Computer-Aided Civil and Infrastructure Engineering, 30(7), 508-523.
- FEMA (2003), HAZUS-MH technical manual: earthquake model. Multi hazard loss estimation methodology. United States Department of Homeland Security, Federal Emergency Management Agency, Washington, DC.
- Fragiadakis, M., Vamvatsikos, D., Christodoulou, S.E. (2013). Reliability assessment of urban water distribution networks under seismic loads. Water Resources Management, 27(10), 3739-3764. http://dx.doi.org/10.1007/s11269-013-0378-0
- GEM (2021). The OpenQuake-engine User Manual. Global Earthquake Model, OpenQuake Manual for Engine version 3.12.1. http://dx.doi.org/10.13117/GEM.OPENQUAKE.MAN.ENGINE.3.12.1
- HYPERION (2019). Development of a decision support system for improved resilience and sustainable reconstruction of historic areas to cope with climate change and extreme events based on novel sensors and advanced modelling tools. The HYPERION Consortium, Athens, Greece. URL: https://www.hyperion-project.eu/
- Gibbons, A. (1985). Algorithmic graph theory. Cambridge University Press, Cambridge.
- Hagberg, A.A., Schult, D.A., Swart, P.J. (2008). Exploring network structure, dynamics, and function using NetworkX. In Proceedings of the 7th Python in Science Conference (SciPy2008), Pasadena, CA.
- Jayaram, N., Baker, J.W. (2009). Correlation model for spatially distributed ground-motion intensities. Earthquake Engineering and Structural Dynamics, 38(15), 1687-1708. https://doi.org/10.1002/eqe.922
- Kohrangi, M., Bazzurro, P., Vamvatsikos, D. (2021). Seismic risk and loss estimation for the building stock in Isfahan. Part II: Hazard analysis and risk assessment. Bulletin of Earthquake Engineering, 19: 1739-1763. DOI: 10.1007/s10518-020-01037-1
- Silva, V., Crowley, H., Varum, H., Pinho, R. (2015). Seismic risk assessment for mainland Portugal. Bulletin of Earthquake Engineering, 13(2), 429-457. https://doi.org/10.1007/s10518-014-9630-0
- Tomar, A., Burton, H. V., Mosleh, A., Yun Lee, J. (2020). Hindcasting the Functional Loss and Restoration of the Napa Water System Following the 2014 Earthquake Using Discrete-Event Simulation. Journal of Infrastructure Systems, 26(4), 04020035. https://doi.org/10.1061/(ASCE)IS.1943-555X.0000574
- Winkler, J., Duenas-Osorio, L., Stein, R., & Subramanian, D. (2010). Performance assessment of topologically diverse power systems subjected to hurricane events. Reliability Engineering & System Safety, 95(4), 323-336.